

nantenna

تقديم الطالب جعفر محفوض
إشراف المدرس محمود نوح
السنة الدراسية 2016/2015

Index :

Introduction :	3
Proprties of antanna :	4
Frequency and size	
Directivity	
Radiation pattern	
Physical construction	
Applications	
Kinds of antenna :	7
¼ wavelength ground plane	
Yagi antenna	
Nantenna :	9
The way of fabrication	
Optical characterization of nano-antenna	
Summary :	16
The resourses and edocumentation :	17

Introduction :

The development of the communication systems comes from the wide application of these systems in our daily life .

Antennas are found around us in abundance when we are in the midst of communicating either locally or globally via radio frequencies or microwave technologies. Since the inception of classical electromagnetics to the wonders of modern electromagnetism antennas in any size or form have and are still working diligently to uphold their purpose, that is, to convert the electromagnetic energy available in free space into confined electric signals and vice versa. As the telecommunication industry is reaching new technological heights, antennas in any size or form have and are still working diligently to uphold their purpose, that is, to convert the electromagnetic energy available in free space into confined electric signals and vice versa. As the telecommunication industry is reaching new technological heights, the demand for energy consumption is also surging, resulting in an increase in environmental problems in the form of carbon emissions. One proposed solution is the concept of "green communication," which primarily aims at improving the energy efficiency while reducing the CO₂ emissions and energy consumption of communication networks. In order to realize this concept, researchers are now persuaded on designing antennas by utilizing the electromagnetic spectrum in the high frequency bands (THz), which fulfills the bandwidth hunger requirements of smart devices, provides low cost designs with high connectivity, and satisfies the consumer needs while keeping the environment clean and energy consumption to a minimum. The antennas designed in the THz regime are given the name of optical antennas.

And this kind of antenna's applications wasn't just in the communication but it omit this edge and have applications in the solar systems to absorb the light waves . and because of it's range that idecate to fabricate it in nanno dimension .

Properties of Antennas :

- Frequency and size :

antennas used for HF(high frequency) are different from the ones used for VHF(very high frequency), which in turn are different from antennas for microwave. The wavelength is different at different frequencies, so the antennas must be different in size to radiate signals at the correct wavelength. We are particularly interested .

in antennas working in the microwave range, especially in the 2.4 GHz and 5 GHz frequencies. At 2.4 GHz the wavelength is 12.5 cm, while at 5 GHz it is 6 cm.

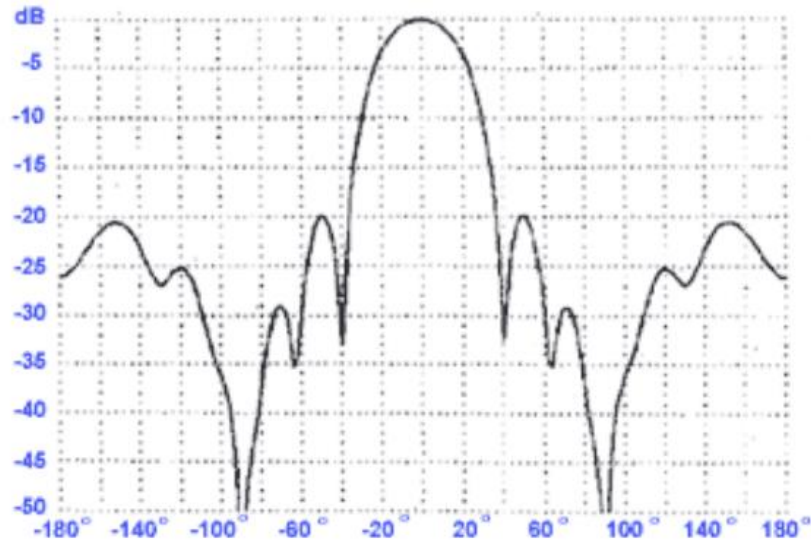
- Directivity :

antennas can be omnidirectional, sectorial or directive. Omnidirectional antennas radiate the same pattern all around the antenna in a complete 360 degrees pattern. The most popular types of omnidirectional antennas are the Dipole-Type and the Ground Plane. Sectorial antennas radiate primarily in a specific area. The beam can be as wide as 180 degrees, or as narrow as 60 degrees. Directive antennas are antennas in which the beamwidth is much narrower than in sectorial antennas. They have the highest gain and are therefore used for long distance links. Types of directive antennas are the Yagi, the biquad, the horn, the helicoidal, the patch antenna, the Parabolic Dish and many others.

- Radiation Pattern :

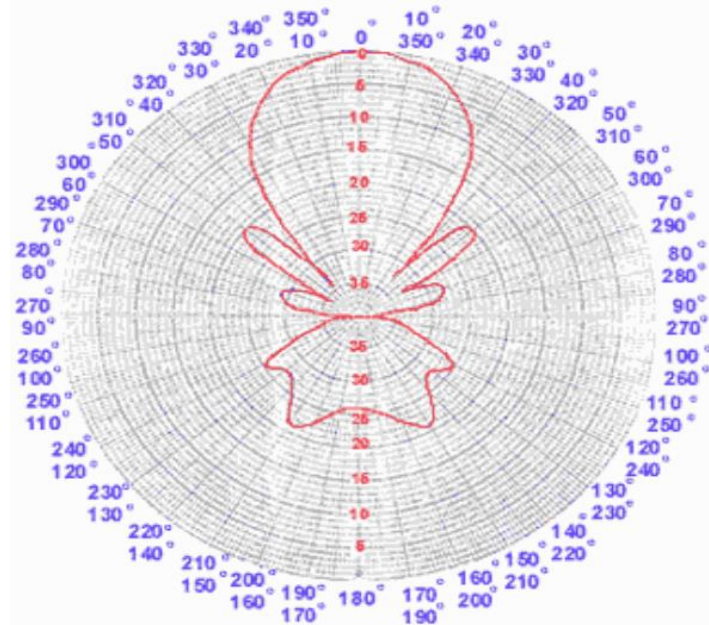
The radiation or antenna pattern describes the relative strength of the radiated field in various directions from the antenna, at a constant distance. The radiation pattern is a reception pattern as well, since it also describes the receiving properties of the antenna. The radiation pattern is three-dimensional, but usually the measured radiation patterns are a two dimensional slice of the three-dimensional pattern, in the horizontal or vertical planes. These pattern measurements are presented in either a *rectangular* or a *polar* format. The following figure shows a rectangular plot presentation of a typical 10 element Yagi. The detail is good but it is difficult to visualize the antenna behavior at different directions.

Graph 1



Polar coordinate systems are used almost universally. In the polar coordinate graph, points are located by projection along a rotating axis (radius) to an intersection with one of several concentric circles. Following is a polar plot of the same 10 element Yagi antenna.

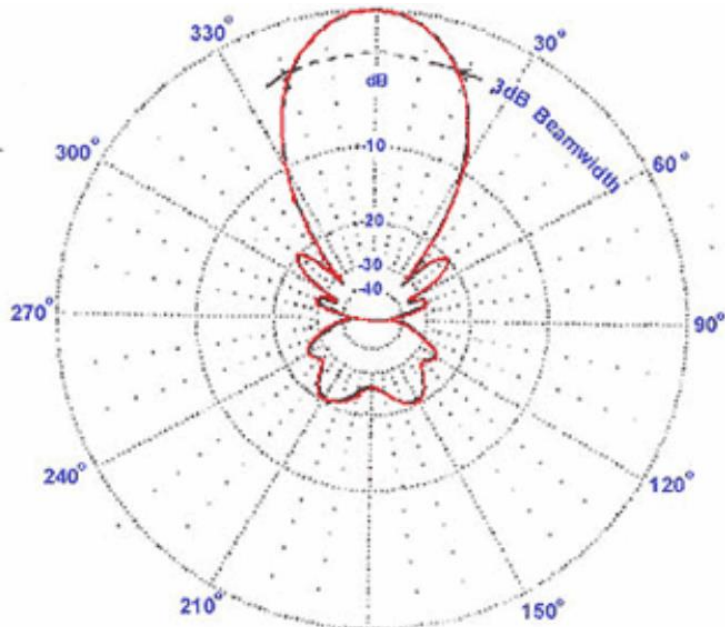
Graph 2



Polar coordinate systems may be divided generally in two classes: *linear* and *logarithmic*. In the linear coordinate system, the concentric circles are equally spaced, and are graduated. Such a grid may be used to prepare a linear plot of the power contained in the signal. For ease of comparison, the equally spaced concentric circles may be replaced with appropriately placed circles representing the decibel response, referenced to 0 dB at the outer edge of the plot. In this kind of plot the minor lobes are suppressed. Lobes with peaks more than 15 dB or so below the main lobe disappear because of their small size. This grid enhances plots in which the

antenna has a high directivity and small minor lobes. The voltage of the signal, rather than the power, can also be plotted on a linear coordinate system. In this case, too, the directivity is enhanced and the minor lobes suppressed, but not in the same degree as in the linear power grid. In the logarithmic polar coordinate system the concentric grid lines are spaced periodically according to the logarithm of the voltage in the signal. Different values may be used for the logarithmic constant of periodicity, and this choice will have an effect on the appearance of the plotted patterns. Generally the 0 dB reference for the outer edge of the chart is used. With this type of grid, lobes that are 30 or 40 dB below the main lobe are still distinguishable. The spacing between points at 0 dB and at -3 dB is greater than the spacing between -20 dB and -23 dB, which is greater than the spacing between -50 dB and -53 dB. The spacing thus correspond to the relative significance of such changes in antenna performance.

Graph 3



A modified logarithmic scale emphasizes the shape of the major beam while compressing very low-level (>30 dB) sidelobes towards the center of the pattern.

There are two kinds of radiation pattern: absolute and relative. Absolute radiation patterns are presented in absolute units of field strength or power. Relative radiation patterns are referenced in relative units of field strength or power. Most radiation pattern measurements are relative to the isotropic antenna, and then the gain transfer method is then used to establish the absolute gain of the antenna.

The radiation pattern in the region close to the antenna is not the same as the pattern at large distances. The term near-field refers to the field pattern that exists close to the antenna, while the term far-field refers to the field pattern at large distances. The far-field is also called the radiation field, and is what is most commonly of interest. Ordinarily, it is the

radiated power that is of interest, and so antenna patterns are usually measured in the far-field region. For pattern measurement it is important to choose a distance sufficiently large to be in the far-field, well out of the near-field. The minimum permissible distance depends on the dimensions of the antenna in relation to the wavelength. The accepted formula for this distance is:

$$r_{min} = \frac{2d^2}{\lambda}$$

where r_{min} is the minimum distance from the antenna, d is the largest dimension of the antenna, and λ is the wavelength

- Physical construction :

antennas can be constructed in many different ways, ranging from simple wires to parabolic dishes, up to coffee cans.

When considering antennas suitable for 2.4 GHz WLAN use, another classification can be used .

- Application :

we identify two application categories which are Base Station and Point-to-Point. Each of these suggests different types of antennas for their purpose.

Base Stations are used for multipoint access. Two choices are Omni antennas which radiate equally in all directions, or Sectorial antennas, which focus into a small area. In the Point-to-Point case, antennas are used to connect two single locations together. Directive antennas are the primary choice for this application. A brief list of common type of antennas for the 2.4 GHz frequency is presented now, with a short description and basic information about their characteristics.

Kinds of antenna :

1/4 Wavelength Ground Plane :

The 1/4 Wavelength Ground Plane antenna is very simple in its construction and is useful for communications when size, cost and ease of construction are important. This antenna is designed to transmit avertically polarized signal. It consists of a 1/4 wave element as half-dipole and three or four 1/4 wavelength ground elements bent 30 to 45 degrees down. This set of elements, called *radials*, is known as a *ground plane*.

This is a simple and effective antenna that can capture a signal equally from all directions. To increase the gain, however, the signal can be flattened out to take away focus from directly above and below, and providing more focus on the horizon. The vertical beamwidth represents the degree of flatness in the focus. This is useful in a Point-to-Multipoint situation, if all the other antennas are also at the same height. The gain of this antenna is in the order of 2 - 4 dBi.

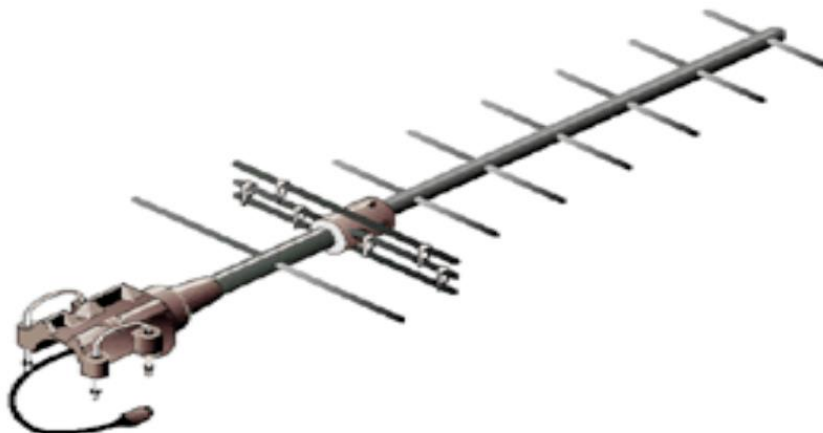
Picture 1



Yagi antenna :

A basic Yagi consists of a certain number of straight elements, each measuring approximately half wavelength. The driven or active element of a Yagi is the equivalent of a center-fed, half-wave dipole antenna. Parallel to the driven element, and approximately 0.2 to 0.5 wavelength on either side of it, are straight rods or wires called reflectors and directors, or passive elements altogether. A reflector is placed behind the driven element and is slightly longer than half wavelength; a director is placed in front of the driven element and is slightly shorter than half wavelength. A typical Yagi has one reflector and one or more directors. The antenna propagates electromagnetic field energy in the direction running from the driven element toward the directors, and is most sensitive to incoming electromagnetic field energy in this same direction. The more directors a Yagi has, the greater the gain. As more directors are added to a Yagi, however, it becomes longer. Following is the photo of a Yagi antenna with 6 directors and one reflector.

picture2



Yagi antennas are used primarily for Point-to-Point links, have a gain from 10 to 20 dBi and a horizontal beamwidth of 10 to 20 degrees.

Nantenna:

nantenna (//**nano antenna**) is a nanoscopic rectifying antenna, an experimental technology being developed to convert light to electric power. The concept is based on the rectenna (rectifying antenna), a device used in wireless power transmission. A rectenna is a specialized radio antenna which is used to convert radio waves into direct current electricity. Light is composed of electromagnetic waves like radio waves, but of much smaller wavelength. A nantenna is a very small rectenna the size of a light wave, fabricated using nanotechnology, which acts as an "antenna" for light, converting light into electricity. It is hoped that arrays of nantennas could be an efficient means of converting sunlight into electric power, producing solar power more efficiently than conventional solar cells.

The idea was first proposed by Robert L. Bailey in 1972. As of 2012, only a few nantenna devices have been built, demonstrating only that energy conversion is possible. It is unknown if they will ever be as cost-effective as photovoltaic cells. A nantenna is an electromagnetic collector designed to absorb specific wavelengths that are proportional to the size of the nantenna. Currently, Idaho National Laboratories has designed a nantenna to absorb wavelengths in the range of 3–15 μm . These wavelengths correspond to photon energies of 0.08 - 0.4 eV. Based on antenna theory, a nantenna can absorb any wavelength of light efficiently provided that the size of the nantenna is optimized for that specific wavelength. Ideally, nantennas would be used to absorb light at wavelengths between 0.4 and 1.6 μm because these wavelengths have higher energy than far-infrared (longer wavelengths) and make up about 85% of the solar radiation spectrum.

As optical counterpart of microwave antennas, optical nano-antennas are important devices for converting propagating radiation into confined/enhanced fields at nanoscale. The recent advances in resonant sub-wavelength optical antennas have now offered researchers a continuum of electromagnetic spectrum—from radio frequencies all the way up to X-rays—to design, analyze and predict new phenomena that were previously unknown. Their applications in areas with pressing needs, e.g., in sensing, imaging, energy harvesting, and disease cure and prevention, have brought revolutionary improvements. This research gives important characteristics of these plasmonic* resonators through optical and electron-beam excitation using nanostructures defined by lithography as well as a newly developed direct metal patterning technique.

The important challenges in optical antenna research include both fundamental understanding of the underlying physics as well as issues related to fabrication of low cost, high throughput nanostructures beyond the diffraction limit. The nanoscale feature size of optical antennas limits our ability to design, manufacture, and characterize their resonant behavior. In this regard, how electron-beam lithography can be coupled with a new solid-state electrochemical process to directly pattern metal nanostructures with possibility of sub-10 nm features at low cost, minimal infrastructure, and ambient conditions.

* a quantum associated with a local collective oscillation of charge density

Using bowtie antennas as representative of the general class of optical nanoantennas, these research shows how optical imaging can be used as a simple tool to characterize their resonant behavior. Further understanding of their spatial and spectral modes is gathered using finite-difference time domain simulations. The extremely high fields generated in gaps of closely coupled bowties are used in non-linear signal generation and several sumfrequency phenomena are identified.

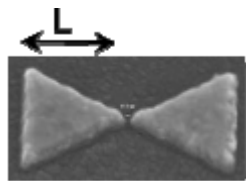
The sub-wavelength confinement of fields in optical antennas requires new techniques that can image beyond diffraction limited optical imaging. One such technique, cathodoluminescence (CL) imaging spectroscopy, which has been demonstrated to resolve sub-25 nm antenna modes, is used to map various modes of triangular and bowtie antennas. The highly localized electron-beam in CL is used to excite and map the hybridized modes of bowtie dimers, including anti-parallel “dark” modes. These high quality dark modes are critical for overcoming the fundamental limitations associated with wideband resonances in plasmonic resonators.

An optical nano-antenna is a noble metal nanostructure that can sustain electron-plasma oscillations leading to a resonant frequency that is proportional to its characteristic size L , and index of surrounding medium n . Similar to a microwave dipole,

the resonant wavelength is given by $\lambda_{res} = 2 \cdot n \cdot L$.

the resonant wavelength λ_{res} is dependent on type of metal (through λ_p , the plasmon frequency), antenna geometry, and the dielectric properties of the surrounding medium.

Another way to “engineer” the antenna properties is by using a dimer antenna and varying the gap between the particles.



picture3

The way of fabrication :

Electron-beam lithography :

Electron-beam lithography is one of the most common techniques to fabricate sub-100 nm features. Since this technique is highly matured and has been extensively used, only a general overview of fabrication steps is provided

For samples fabricated for optical measurements, gold and silver nano-antennas were fabricated on 0.4 mm thick glass substrates with 25 nm thick ITO coating (CEC080P from PraezisionsGlas & Optik GmbH, Germany). Samples for cathodoluminescence measurements were fabricated on 2 inch prime grade Si(100) substrates (from www.Universitywafers.com).

The pre-cleaned substrates were first sonicated in an acetone bath for 5 min and dried at 200 °C for 2 min. Afterwards, Poly(methyl methacrylate) (PMMA) photoresist (2% solution of 95k mol. wt. in anisoline, from MicroChem Corp.) was spin deposited at 2000 RPM for 60 sec. The polymer was baked for 2 minutes at 200 °C resulting into ~ 90 nm thick resist layer. The e-beam lithography exposure was carried out at 20 nA beam current at various dose values. After exposure, the samples were developed for 180 sec in 3:1 solution of IPA:MIBK. All the silver samples were fabricated using e-beam evaporation (Cooke Evaporator) in the Micro and Nano Technology Lab at pressures below 8E-7 torr, with a 3 nm Cr adhesion layer underneath. The gold samples were fabricated with e-beam evaporators (Temescal) in the Materials Research Lab at pressures ~ 5E-6 torr, with 3 nm Ti adhesion layer. Finally, acetone was used for lift-off, followed by sonication in steps of 30 sec (but only when found necessary).

Solid-state superionic stamping (S4) :

Hsu et al. [47-50] have previously reported a novel method of direct metal patterning using electrochemical etching with a superionic conductor “stamp.” A stamp was brought in contact with metal film and small external potential (~0.3 V) and low pressure (< 10 MPa) were applied. Etching of the metal film at the contact region resulted in a metal pattern complementary to the original stamp.

To effectively excite the nano-antennas, narrow gaps with precise control of the features are critical, with the ability to fabricate them over large areas. To overcome these constraints in S4, which is limited by the FIB-milling process, a new approach based on embossing was taken. The procedure and representative images during the various steps of the modified S4 are shown in Fig 1 .

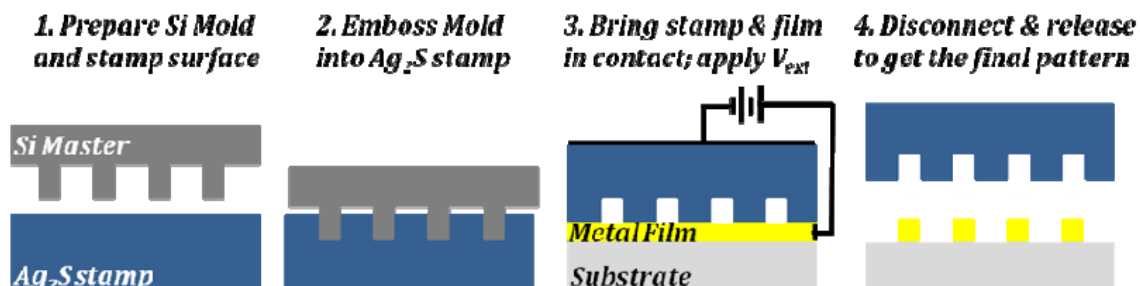


Fig 1

To summarize the process, Si molds were fabricated using e-beam lithography and reactive-ion etching (Step 1). This mold is then embossed into Ag₂S (Step 2) to generate a complementary pattern.

Finally, the stamp fabricated using embossing is used for the direct metal etching of Ag film (Steps 3 and 4).

Improving silver film quality :

Silver is currently the most important plasmonic material for optical devices including optical antennas. Due to its lower bulk electrical resistivity ($1.57 \mu\text{cm}$ at room temperature) and resistance to electromigration in metal interconnects, silver is also a potential material for achieving higher current densities and faster switching speeds.

Despite several decades of efforts, there exists a lack of control over film growth of silver films, due to its high mobility and island-like growth. Therefore, improving device performance by growing high quality films is of enormous interest. A new approach of improving the Ag film roughness by depositing a very thin Ge buffer layer has been shown earlier, which changes the thermodynamics of film growth. Here, a new approach using MgO buffer layer, which has very small lattice mismatch with Ag, is used that allows epitaxial growth of very thin metal films with extremely low roughness. Besides metal films, metal-oxide structures are important in several applications including metal-oxide-semiconductor field-effect transistors (MOS-FET), magnetic tunneling junctions (in magnetoelectronics and magnetic data storage), and in oxide heterostructures, as well as in catalysts, corrosion resistance coatings and sensors. MgO is specifically suited due to the large band-gap of 7.8 eV, it has been shown that epitaxially grown MgO films as thin as three monolayers can maintain a high band gap of up to 6 eV [63]. Additionally, MgO has low dielectric constant ($n=1.7$), low optical loss, excellent high-temperature chemical stability as well as excellent thermal conductance.

The Ag-MgO system is specifically interesting due to very low lattice mismatch (<3%), which is expected to result in reduced defects and more uniform films.

Therefore, Ag films grown on MgO should offer improved film quality as well as a better metal-dielectric combination. However, low lattice mismatch is no guarantee for smooth films since silver films on MgO (or in general metal films on oxides) grow by Volmer-Weber mode (i.e., island-like growth). This is a serious concern for silver films due to the very high mobility of adsorbed Ag adatoms. The important drawbacks of this are higher losses in optical nanostructures and enhanced resistivity due to scattering in electronic devices. Besides these limitations, the quality of both the MgO and MgO/Ag films can be dramatically improved by using a very thin (0.1-1 nm) silver layer on top of the Si/SiO₂ substrate. This is confirmed using morphological studies of the films using AFM, and large area uniformity of the films using X-ray reflectivity. Since electronic devices are susceptible to temperature fluctuations, effect of annealing on the MgO/Ag films is also studied.

Silver and MgO films were deposited using electron-beam evaporation at a rate of 0.5 Å/s and base pressure of 5×10^{-6} Torr. MgO was purchased from Kurt J. Lesker as fused pieces (99.95% purity) and was evaporated without any oxygen

atmosphere. Prior to deposition, the Si(100) substrates were cleaned using acetone, deionized water, and ethyl-alcohol, and blow-dried using nitrogen. No additional cleaning or removal of the native oxide was performed.

AFM measurements were performed on a Digital Instruments/ Veeco Dimension 3100 atomic force microscope with standard tips. The X-ray reflectivity measurements were carried out using a state-of-the-art modular 'Xpert' XRD system (from Philips) mounted with Cu X-ray source. A slit width of 1 mm was used for all the measurements.

For resistivity measurements at elevated temperatures, annealing of the films was carried out in an RTP setup (from ULVAC) with a base pressure of 7×10^{-7} Torr and a rise time of 3 minutes to reach the maximum temperature.

AFM :

Due to the small lattice mismatch between silver ($d = 4.09$ Å) and MgO ($d = 4.21$ Å) minimal strain is expected as the top layer grows. However, several parameters affect the film growth, and lattice mismatch alone may not guarantee better film quality.

In general, direct growth on Si without a native oxide layer is usually not possible and a thin oxide layer forms during sample loading and pump-down even on HF cleaned substrates. From Ag growth perspective, the presence of the oxide layer has no significance since the substrate will only affect the initial mismatched MgO growth of a few monolayers. To understand the behavior of MgO film growth, several different thicknesses were deposited to understand the MgO film quality on Si/SiO₂ substrate.

AFM scans of 3 to 15 nm MgO films show that the thicker films tend to have larger grains with a peak-to-valley size changing from 2.32 nm (3 nm MgO) to 4.59 nm (15 nm MgO). Similarly, the roughness increases from 0.42 nm to 1.41 nm. When silver is deposited on top of these films, they further increase the film roughness as shown in AFM scans of Fig. 2.6 for a 15 nm Ag film on 15 nm MgO layer. The granular films with high pin-hole density have roughness of 5.01 nm and peak-to-valley difference of about 22.20 nm. These values are almost double that observed for a 15 nm Ag film directly deposited onto Si/SiO₂ substrate.

Introduction of a very thin Ag layer (0.1-1 nm) underneath the MgO layer dramatically changes the film properties. As seen in the surface scans of Fig. 2.6, a 20 nm MgO film on 1 nm Ag layer shows very small particle size (peak-to-valley size of 1.62) and an almost six-fold improvement in the film roughness (0.30 nm), thereby making these films more dense and smoother than the original films. When a 15 nm silver film is deposited on such an Ag/MgO multilayer structure, the overall properties of the silver films improve and are confirmed with XRR measurements. To understand the role of the thin Ag layer underneath MgO, 0.5 nm Ag film on Si/SiO₂ substrate was deposited. Due to high mobility and island-like growth of Ag, a discontinuous film with islands as tall as 8-10 nm and particle diameter in the range of 10-50 nm was observed. Therefore, MgO films grown on this base layer have an interface that is a combination of Ag and SiO₂, which seems to provide large nucleation sites and inhibition of particle growth.

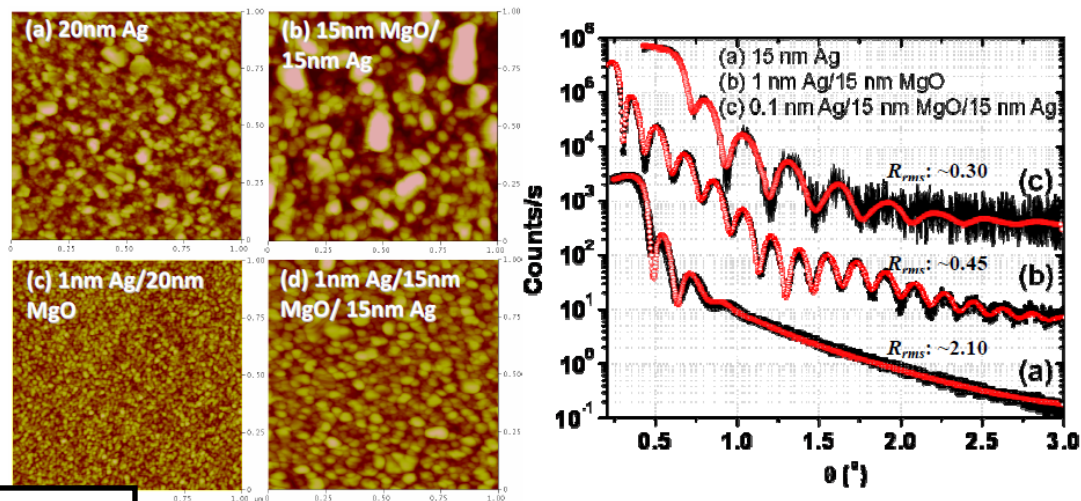


Fig 2

Improving Ag thin film quality using MgO buffer layer. (Left) small area AFM scans with different topography dependent on the MgO buffer layer. (Right) X-ray reflectivity measurements indicating long range order in the films.

OPTICAL CHARACTERIZATION OF NANO-ANTENNAS :

The collective oscillation of electrons in noble metal nanostructures, called localized surface plasmon polaritons (SPPs), are characterized by strong interaction of the conduction electrons with incident radiation. This interaction, at their resonance frequency, results in strong scattering, absorption and local field enhancement near the nanostructures. The process of scattering and absorption involves slow dephasing of the optical polarization associated with the electron oscillation. Consequently, the decay of the plasmons into photons occurs either through emission of photons (radiative process) or loss to electron-hole excitation (non-radiative process). Reducing the nonradiative losses means emission of photons can be maximized and the highest field enhancement can be achieved with the optical polarization. When measured using standard optical spectroscopy, these processes result in a dip in the transmission spectrum and a strong near-field enhancement around the nanostructures.

Most efforts are therefore focused on understanding the behavior of a given system through optical measurements complemented with simulations. Once characterized, this approach allows application of the localized SPPs in a wide range of applications including surface enhanced Raman spectroscopy [24, 71] and non-linear spectroscopy. The enhanced fields are specifically important for processes involving sum frequency generation since the resulting high photon densities increase the probability of photon combination. Therefore, optical characterization is the first step in understanding the nature of particle resonance, near-field distribution and possible applications in various areas including non-linear spectroscopy.

Antenna extinction cross section :

For any optical studies, the first step in characterization of antennas involves excitation of the nanostructures using a broadband source. The transmitted signal shows a dip in the spectrum corresponding to the antenna resonance.

At this wavelength, the incoming radiation has the highest coupling with the structures. To quantify the quality of this interaction, the most common method is to measure the scattering cross section, which is related to the ability of the antenna to scatter, absorb and reradiate the incoming radiation. A large cross section means high interaction volume of the nanostructure, providing better sensitivity to the nearby molecules and other species used for sensing. During optical measurements, the transmitted intensity I at the spectrometer is a function of the incident beam power, and absorption and scattering by the antenna at each wavelength, which can be expressed as

$$I(\lambda) = I_{inc}(\lambda) - I_{abs}(\lambda) - I_s(\lambda)$$

where I_{inc} is the intensity of the incident beam, I_{abs} is the intensity loss due to absorption in the antenna, and I_s is the intensity loss due to scattering in all directions.

Antenna scaling laws :

For designing antennas with appropriate resonance wavelengths, experiments were performed on lithographically fabricated nanostructures with various sizes. It relates the resonant wavelength with triangle length (tip-to-opposite edge) of bowties and the substrate index, $\lambda_{res} = 2 * n * L$. The actual system is more complex due to the presence of 25 nm ITO ($n=1.95$) and the coupling between the triangles. However, the observed slope is comparable to RF dipoles, suggesting this simple relationship holds for these nanostructures at near-IR wavelength range, as suggested earlier.

Polarization dependence:

Triangular structures are polarization independent; however, bowties show a strong dependence on polarization of the applied field. The two main polarizations, along bowtie axis and normal to axis, will excite different modes. Polarization along the long axis will result in strong interaction between the two triangles leading to a stronger and red-shifted peak. This polarization also results in very high fields in the gap due to strong charge interactions at the tips of the triangles. However, for normal polarization the tips at the gap have minimal contribution to charge oscillations resulting in resonance behavior similar to two independent triangles.

Summary :

At the end of this research we could see that the nano techno development of the antenna could move us from a new communication application into new solar system that we could use in the wild energy applications . and that the nano structure application properties added new qualifications to this antenna . like the range of the absorbed wavelength .

There is two main ways of fabrication these antennas .

This kind of tools is still improving and the labrotarys are trying to put the application of this antennas in our daily work .

Sources :

- KUMAR, A. (2011). OPTICAL NANO-ANTENNAS: FABRICATION, CHARACTERIZATION AND APPLICATIONS. University of Illinois at Urbana-Champaign.
- Chaitali Ingale, T. I., Anand Trikolikar (March-April 2013). "Study of Different Types of Microwave Antenna and Its Applications." International Journal of Computer Technology and Electronics Engineering: 4.

Photo index :

The name	Explain	Page number
Graph 1	Rectangular format	5
Graph 2	Polar format	5
Graph 3	Example for polar format	6
Picture 1	$\frac{1}{4}$ wavelength ground plane	8
Picture 2	Yagi antenna	8
Picture 3	Nantenna	10
Fig 1	S(4) steps	11
Fig 2	x-ray reflectiity	14